The X-ray Structure of a Transition State Analog Complex Reveals the Molecular Origins of the Catalytic Power and Substrate Specificity of Acetylcholinesterase

Michal Harel,[†] Daniel M. Quinn,[‡] Haridasan K. Nair,[‡,§] Israel Silman,[⊥] and Joel L. Sussman*,[†,||]

Contribution from the Departments of Structural Biology and Neurobiology, Weizmann Institute of Science, Rehovot 76100, Israel, Biology and Chemistry Departments, Brookhaven National Laboratory, Upton, New York 11973, and Department of Chemistry, University of Iowa, Iowa City, Iowa 52242

Received July 7, 1995[⊗]

Abstract: The structure of a complex of *Torpedo californica* acetylcholinesterase with the transition state analog inhibitor *m*-(*N*,*N*,*N*-trimethylammonio)-2,2,2-trifluoroacetophenone has been solved by X-ray crystallographic methods to 2.8 Å resolution. Since the inhibitor binds to the enzyme about 10^{10}-fold more tightly than the substrate acetylcholine, this complex provides a visual accounting of the enzyme−ligand interactions that provide the molecular basis for the catalytic power of acetylcholinesterase. The enzyme owes about 8 kcal mol^{-1} of the 18 kcal mol^{-1} of free energy of stabilization of the acylation transition state to interactions of the quaternary ammonium moiety with three water molecules, with the carboxylate side chain of E199, and with the aromatic side chains of W84 and F330. The carbonyl carbon of the trifluoroketone function interacts covalently with S200 of the S200−H440−E327 catalytic triad. The operation of this triad as a general acid−base catalytic network probably provides 3−5 kcal mol^{-1} of the free energy of stabilization of the transition state. The remaining 5−7 kcal mol^{-1} of transition state stabilization probably arises from tripartite hydrogen bonding between the incipient oxyanion and the NH functions of G118, G119, and A201. The acetyl ester hydrolytic specificity of the enzyme is revealed by the interaction of the CF_3 function of the transition state analog with a concave binding site comprised of the residues G119, W233, F288, F290, and F331. The highly geometrically convergent array of enzyme−ligand interactions visualized in the complex described herein envelopes the acylation transition state and sequesters it from solvent, this being consistent with the location of the active site at the bottom of a deep and narrow gorge.

Introduction

The principal role of acetylcholinesterase (AChE,[1] acetylcholine hydrolase, EC 3.1.1.7) is termination of impulse transmission at cholinergic synapses by rapid hydrolysis of the neurotransmitter acetylcholine (ACh).[2,3] In keeping with this requirement, AChE possesses a remarkably high specific activity, especially for a serine hydrolase,[4] functioning under bimolecular conditions at a rate approaching the diffusion-controlled limit.[5−7] Kinetic studies indicated that the active site of AChE consists of two major subsites, the "esteratic" and "anionic" subsites, corresponding to the catalytic machinery and the choline binding pocket, respectively.[8] Elucidation of the three-dimensional structure of *Torpedo californica* AChE (TcAChE) by Sussman *et al*.[9] confirmed earlier studies, and showed that AChE contains a catalytic triad similar to that present in other serine hydrolases.[10−13] Unexpectedly, it has also revealed that this triad is located near the bottom of a deep and narrow cavity, *ca*. 20 Å deep, named the "aromatic gorge", since it is lined by the rings of 14 highly conserved aromatic residues.[14] Certain of these conserved aromatic residues play important roles in both the esteratic and aromatic subsites.[15−19]

The crystallographic data obtained so far, taken together with chemical modification,[19,20] site-directed mutagenesis,[21−25] molecular modeling,[9,21−26] and kinetic and spectroscopic stud-

* To whom correspondence should be addressed at the Weizmann Institute. FAX: 972-8-344159. E-mail: joel@sgjs3.weizmann.ac.il.
[†] Department of Structural Biology, Weizmann Institute of Science.
[‡] University of Iowa.
[§] Current address: Clarion Pharmaceuticals, 585 Science Dr., Madison, WI 53711.
[⊥] Department of Neurobiology, Weizmann Institute of Science.
[||] Brookhaven National Laboratory.
[⊗] Abstract published in *Advance ACS Abstracts,* February 15, 1996.

(1) Abbreviations: ACh, acetylcholine; AChE, acetylcholinesterase; ATCh, (acetylthio)choline; EDR, edrophonium; TcAChE, *Torpedo californica* AChE. Single letter amino acid codes used: A, alanine; C, cysteine; D, aspartate; E, glutamate; F, phenylalanine; G, glycine; H, histidine; L, leucine; S, serine; V, valine; W, tryptophan; Y, tyrosine. The sequence numbering of TcAChE is used throughout this paper when amino acid residues of any AChE are discussed.

(2) Rosenberry, T. L. *Adv. Enzymol. Relat. Areas Mol. Biol.* **1975**, *43*, 103−218.
(3) Taylor, P. In *Pharmacological Basis of Therapeutics*; Gilman, A. G., Goodman, L. S., Murad, F., Eds.; MacMillan: New York, 1985; pp 110−129.
(4) Quinn, D. M. *Chem. Rev.* **1987**, *87*, 955−979.
(5) Bazelyansky, M.; Robey, E.; Kirsch, J. F. *Biochemistry* **1986**, *25*, 125−130.
(6) Hasinoff, B. B. *Biochim. Biophys. Acta* **1982**, *704*, 52−58.
(7) Nolte, H.-J.; Rosenberry, T. L.; Neumann, E. *Biochemistry* **1980**, *19*, 3705−3711.
(8) Froede, H. C.; Wilson, I. B. In *The Enzymes*, 3rd ed.; Boyer, P. D., Ed.; Academic Press: New York, 1971; Vol. 5, pp 87−114.
(9) Sussman, J. L.; Harel, M.; Frolow, F.; Oefner, C.; Goldman, A.; Toker, L.; Silman, I. *Science* **1991**, *253*, 872−879.
(10) Stroud, R. M. *Sci. Am.* **1974**, *231*, 74−88.
(11) Blow, D. M. *Acc. Chem. Res.* **1976**, *9*, 145−152.
(12) Kraut, J. *Annu. Rev. Biochem.* **1977**, *46*, 331−358.
(13) Polgar, L. In *Hydrolytic Enzymes*; Neuberger, A., Brocklehurst, K., Eds.; Elsevier: Amsterdam, 1987; pp 159−200.
(14) Gentry, M. K.; Doctor, B. P. In *Cholinesterases: Structure, Function, Mechanism, Genetics, and Cell Biology*; Massoulié, J., Bacou, F., Barnard, E., Chatonnet, A., Doctor, B. P., Quinn, D. M., Eds.; American Chemical Society: Washington, DC, 1991; pp 394−398.
(15) Sussman, J.; Harel, M.; Silman, I. In *Membrane Proteins: Structures, Interactions and Models*; Pullman, A., *et al*., Eds.; Kluwer Academic Publishers: The Netherlands, 1992; pp 161−175.

0002-7863/96/1518-2340$12.00/0

Scheme 1

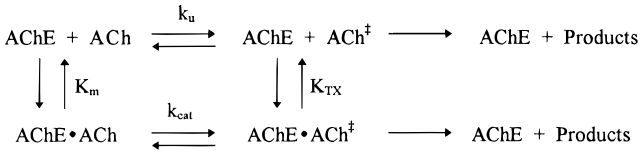

ies,[2−4,8,27,28] yield important insights into the putative involvement of various amino acid residues in substrate recognition and hydrolysis. A crystallographic view of a catalytically relevant complex has, however, been lacking. The availability of such a complex can not only verify the correctness of the above-mentioned experimental approaches but also suggest additional avenues for structure−function experimentation.

The catalytic power of enzymes has long been attributed to specific interactions with the substrate in the transition state.[29−31] A quantitative measure of the cumulative strength of these interactions can be achieved by utilizing the logic of the thermodynamic cycle,[32] as outlined in Scheme 1. Thus, one can estimate the affinity of AChE for the transition state from the catalytic acceleration that the enzyme brings to bear on ACh turnover. According to transition state theory,[33] the transition state of a reaction, denoted by the superscript ‡ in Scheme 1, is in statistical thermodynamic equilibrium with the reactants. For the nonenzymic (k_u) and AChE-catalyzed (k_{cat}) hydrolyses of ACh, the relevant expressions are the following, where k and h are Boltzmann's and Planck's constants, respectively, and $K_u^{\ddagger}$ and $K_{cat}^{\ddagger}$ are the respective equilibrium constants from which 1 degree of vibrational freedom, that for reaction coordinate motion, has been factored:

$$k_u = (kT/h)K_u^{\ddagger} \quad (1)$$

$$k_{cat} = (kT/h)K_{cat}^{\ddagger} \quad (2)$$

The constant for dissociation of the substrate portion of the transition state from AChE, K_{TX}, is derived by utilizing eqs 1 and 2 and the thermodynamic cycle among reactants and transition states in Scheme 1:

$$K_{TX} = K_m K_u^{\ddagger}/K_{cat}^{\ddagger} = K_m k_u/k_{cat} \quad (3)$$

K_m is the Michaelis constant and k_{cat} and k_u are the respective rate constants for the AChE-catalyzed and spontaneous, nonenzymic hydrolyses of ACh. K_{TX}, calculated from the estimated catalytic acceleration wrought by AChE, $k_{cat}/k_u = 10^{13}$, and $K_m = 0.1$ mM,[4,34] is 10 aM. This unusually high biological affinity must arise from numerous geometrically convergent and simultaneous interactions between AChE and ACh in the transition state that are the sources of the catalytic power of the enzyme.

Though one cannot produce a crystal structure of an enzyme complexed with its substrate in the transition state, due to the short lifetime of the transition state versus the time required for X-ray data collection, one can exploit the high affinity of transition state analogs.[32,35,36] A number of reports have described transition state analog inhibitors of AChE.[37−41] One such analog, *m*-(*N*,*N*,*N*-trimethylammonio)-2,2,2-trifluoroacetophenone (TMTFA), first reported by Brodbeck *et al.*,[38] has recently been studied in depth.[42,43] The K_i for inhibition of TcAChE by TMTFA is 15 fM, which is lower by only 3 orders of magnitude than the estimated affinity for the transition state, and is about 10 orders of magnitude higher than the affinity of the substrate in the ES complex, as estimated from the K_m. It seemed, therefore, that TMTFA could serve as a ligand of choice for visualizing the important interactions within the active site which are responsible for the remarkable catalytic activity of AChE.

In the following we present the refined crystal structure at 2.8 Å resolution of the covalent complex of TMTFA and TcAChE. This structure faithfully displays many of the features predicted for the transition state of the enzyme reaction and permits us to discuss the contributions of various structural elements to the catalytic power.

Results and Discussion

The 10^{13}-fold catalytic acceleration of ACh hydrolysis effected by AChE corresponds to 18 kcal mol^{-1} of free energy[44] of stabilization of the transition state. The transition state analog

(16) Sussman, J.; Silman, I. *Curr. Opin. Struct. Biol.* **1992**, *2*, 721−729.
(17) Silman, I.; Krejci, E.; Duval, N.; Bon, S.; Chanal, P.; Harel, M.; Sussman, J.; Massoulié, J. In *Multidisciplinary Approaches to Cholinesterase Functions*; Shafferman, A., Velan, B., Eds.; Plenum: New York, 1992; pp 177−183.
(18) Harel, M.; Sussman, J. L.; Krejci, E.; Bon, S.; Chanal, P.; Massoulié, J.; Silman, I. *Proc. Natl. Acad. Sci. U.S.A.* **1992**, *89*, 10827−10831.
(19) Harel, M.; Schalk, I.; Ehret-Sabatier; L.; Bouet, F.; Goeldner, M.; Hirth, C.; Axelsen, P. H.; Silman, I.; Sussman, J. L. *Proc. Natl. Acad. Sci. U.S.A.* **1993**, *90*, 9031−9035.
(20) Weise, C.; Kreienkamp, H. J.; Raba, R.; Pedak, A.; Aaviksaar, A.; Hucho, F. *EMBO J.* **1990**, *9*, 3385−3388.
(21) Shafferman, A.; Kronman, C.; Flashner, Y.; Leitner, M.; Grosfeld, H.; Ordentlich, A.; Gozes, Y.; Cohen, S.; Ariel, N.; Barak, D.; Harel, M.; Silman, I.; Sussman, J. L.; Velan, B. *J. Biol. Chem.* **1992**, *267*, 17640−17648.
(22) Shafferman, A.; Velan, B.; Ordentlich, A.; Kronman, C.; Grosfeld, H.; Leitner, M.; Flashner, Y.; Cohen, S.; Barak, D.; Ariel, N. In *Multidisciplinary Approaches to Cholinesterase Functions*; Shafferman, A., Velan, B., Eds.; Plenum: New York, 1992; pp 165−175.
(23) Radić, Z.; Gibney, G.; Kawamoto, S.; MacPhee-Quigley, K.; Bongiorno, C.; Taylor, P. *Biochemistry* **1992**, *31*, 9760−9767.
(24) Radić, Z.; Pickering, N. A.; Vellom, D. C.; Camp, S.; Taylor, P. *Biochemistry* **1993**, *32*, 12074−12084.
(25) Ordentlich, A.; Barak, D.; Kronman, C.; Flashner, Y.; Leitner, M.; Segall, Y.; Ariel, N.; Cohen, S.; Velan, B.; Shafferman, A. *J. Biol. Chem.* **1993**, *268*, 17083−17095.
(26) Selwood, T.; Feaster, S. R.; States, M. J.; Pryor, A. N.; Quinn, D. M. *J. Am. Chem. Soc.* **1993**, *115*, 10477−10482.
(27) Massoulié, J.; Pezzementi, L.; Bon, S.; Krejci, E.; Vallette, F.-M. *Prog. Neurobiol.* **1993**, *41*, 33−91.
(28) Taylor, P.; Radić, Z. *Annu. Rev. Pharmacol. Toxicol.* **1994**, *34*, 281−320.
(29) Pauling, L. *Am. Sci.* **1948**, *36*, 51−58.
(30) Fersht, A. R. *Proc. R. Soc. London, B* **1974**, *187*, 397−407.
(31) Schowen, R. L. In *Transition States of Biochemical Processes*; Gandour, R. D., Schowen, R. L., Eds.; Plenum: New York, 1978; pp 77−114.
(32) Wolfenden, R. In *Transition States of Biochemical Processes*; Gandour, R. D., Schowen, R. L., Eds.; Plenum: New York, 1978; pp 555−578.
(33) Glasstone, S.; Laidler, K. J.; Eyring, H. *The Theory of Rate Processes*; McGraw-Hill: New York, 1941.
(34) The 10^{13}-fold catalytic acceleration effected by AChE was estimated as the ratio of $k_{cat} = 10^4$ s^{-1} and the rate constant for the neutral hydrolysis of ACh, which was estimated by Schowen as $k_u \cong 8 \times 10^{-10}$ s^{-1}.
(35) Wolfenden, R. *Nature* **1969**, *223*, 704−705.
(36) Lienhard, G. E. *Science* **1973**, *180*, 149−154.
(37) Allen, K. N.; Abeles, R. H. *Biochemistry* **1989**, *28*, 8466−8473.
(38) Brodbeck, U.; Schweikert, K.; Gentinetta, R.; Rottenberg, M. *Biochim. Biophys. Acta* **1979**, *567*, 357−369.
(39) Dafforn, A.; Neenan, J. P.; Ash, C. E.; Betts, L.; Finke, J. M.; Garman, J. A.; Pao, M.; Walsh, K.; Williams, R. R. *Biochem. Biophys. Res. Commun.* **1982**, *104*, 597−602.
(40) Gelb, M. H.; Svaren, J. P.; Abeles, R. H. *Biochemistry* **1985**, *24*, 1813−1817.
(41) Linderman, R. J.; Leazer, J.; Roe, R. M.; Venkatsh, K.; Selinsky, B. S.; London, R. E. *Pest. Biochem. Physiol.* **1988**, *31*, 187−194.
(42) Nair, H. K.; Lee, K.; Quinn, D. M. *J. Am. Chem. Soc.* **1993**, *115*, 9939−9941.
(43) Nair, H. K.; Seravalli, J.; Arbuckle, T.; Quinn, D. M. *Biochemistry* **1994**, *33*, 8566−8576.
(44) Free energy changes were calculated at 298.2 K according to $\Delta\Delta G = -RT \ln(f)$, where f is a numerical factor, such as the catalytic acceleration effected by AChE or the effect of a particular active site mutant.

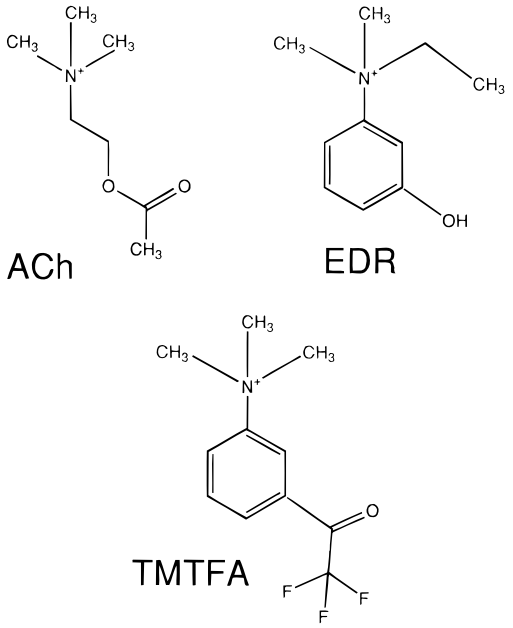

Figure 1. Molecular formulas of acetylcholine (ACh), edrophonium (EDR), and *m*-(*N*,*N*,*N*-trimethylammonio)-2,2,2-trifluoroacetophenone (TMTFA).

complex described herein provides a visual accounting of the interactions that produce this large stabilization energy. Figure 1 shows the formulas of the substrate ACh and the inhibitors TMTFA and edrophonium (EDR). Figure 2 shows the refined structure of the TMTFA−TcAChE complex superimposed on the omit map. Figure 3A displays the position of TMTFA in the active-site gorge in the context of the whole TcAChE structure. Figure 3B shows a model of the tetrahedral intermediate in the acylation stage of ACh[9] turnover superimposed on the experimentally determined TMTFA−TcAChE structure. It can be readily seen that there is remarkable overall similarity between the orientations of the substrate in the model and of the transition state analog in the complex, and that the principal interactions appear to be shared by the two.

The trifluoroketone complex shown in Figures 2 and 3 provides a powerful template for rationalizing various observations in the literature, such as the results of enzyme kinetics, molecular modeling, structure−reactivity, and site-directed mutagenesis experiments. A useful way of organizing a tour through the salient features of the structure is to visit, in turn, various binding loci that make specific contributions to the substrate specificity and catalytic power of AChE. It is in this manner that the following discussion is presented.

Conformation of ACh in the Transition State. Molecular modeling suggested that, in the tetrahedral intermediates generated during the acylation stages of the AChE-catalyzed hydrolyses of ACh[9] and ATCh,[25,26] both substrates are in fully extended conformations. Hence, dihedral angles for both the $Me_3N^+-C-C-X$ (X = O or S) and $C-C-X-COCH_3$ fragments are *ca*. 180°, resulting in projection of the quaternary ammonium function against the open face and π-electron density of the indole group of W84. The bound TMTFA provides a constrained analog of this extended conformation, as shown in Figure 3B by the overlay of the modeled ACh structure and the trifluoroketone transition state analog complex. The experiments of Smissman and co-workers[45−48] suggest that the substrate is also in the extended conformation in the acylation transition state. Constrained acetate esters in which the $R_3N^+-C-C-O$ dihedral angle is approximately *anti* are AChE substrates, whereas those in which the dihedral angle is approximately *gauche* are inhibitors or, at best, very poor substrates. Since ACh is primarily in the *gauche* conformation in solution,[49−52] AChE selects a rare conformation of ACh. Apparently, the advantage of maximizing the quaternary ammonium interaction with W84 overrides the entropic cost of selecting a rare conformation of the substrate. This underscores the importance of the interaction with W84, which is discussed more extensively below. Moreover, TMTFA has a higher affinity for *E. electricus* AChE (K_i = 1.3 fM[42]) than does the noncyclic analog of Abeles and co-workers, $CF_3COCH_2CH_2-CH_2N^+Me_3$ (K_i = 110 fM[37]). The weaker binding of their inhibitor probably arises because, like the substrate ACh, it is not conformationally constrained. AChE must select a single conformation of this inhibitor, and again, the resulting entropic cost would be higher than that required to bind the conformationally constrained TMTFA.

Catalytic Triad and Oxyanion Hole. The catalytic triad of AChE closely resembles that of other serine hydrolases.[9] As Figure 4 illustrates, O^γ of S200 of the triad forms a covalent bond with the carbonyl carbon of TMTFA, which correspondingly assumes a tetrahedral geometry mimicking the tetrahedral intermediate in the acylation stage of catalysis. This covalent interaction accords nicely with the fluorine NMR characteriza-

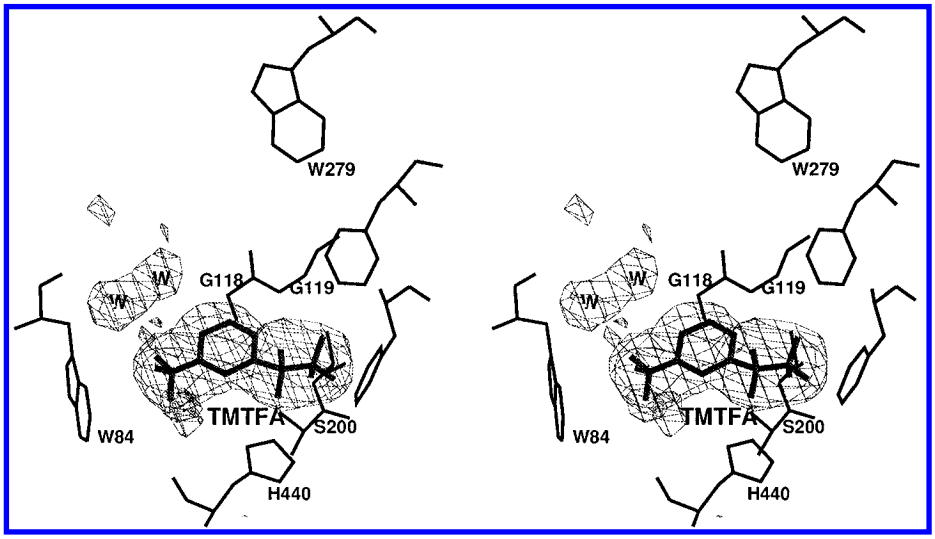

Figure 2. Omit map of the refined structure of the TMTFA−TcAChE complex contoured at 3σ and displayed in stereo. The final refined coordinates are superimposed on the electron density map. Electron density interpreted as water molecules is marked by the letter W. The residue that extends behind the electron density of the bound inhibitor is A201.

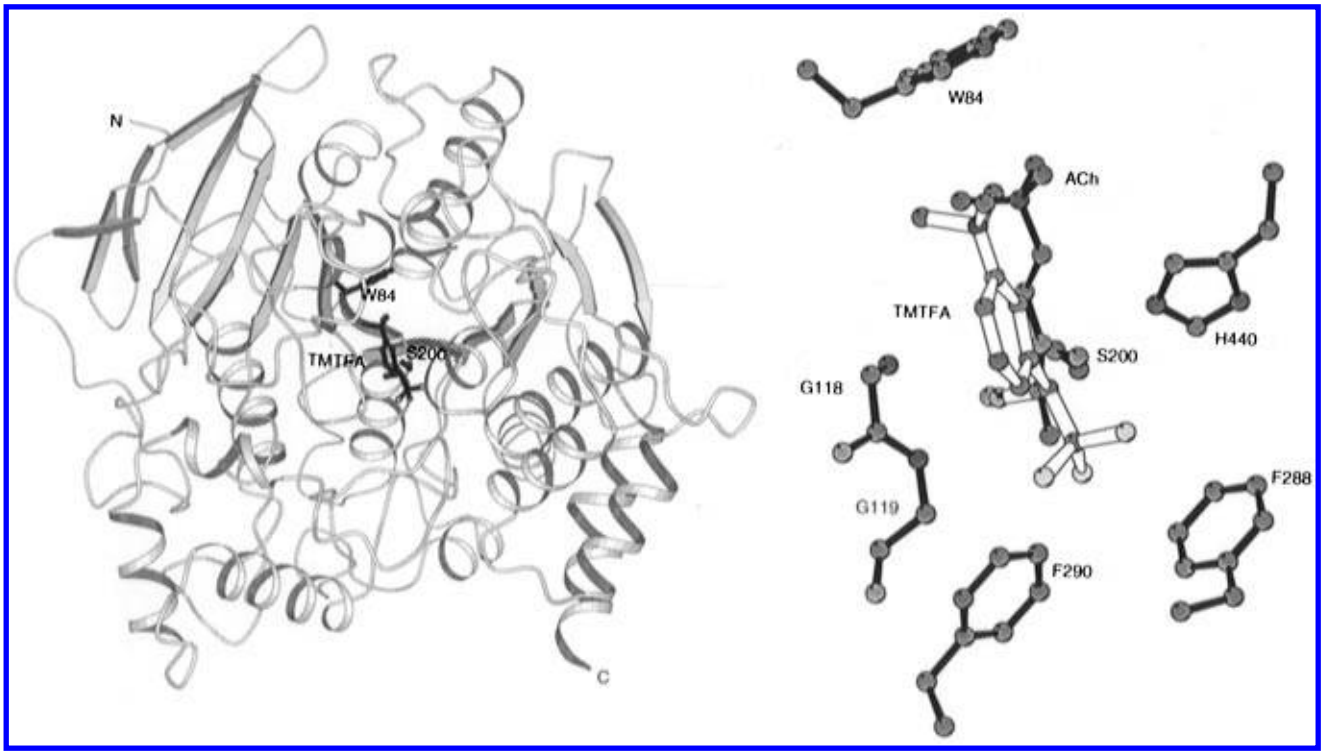

Figure 3. (A, left) Overall conformation of the TMTFA−TcAChE complex. The side chains of S200 of the catalytic triad and of W84, which interacts with the quaternary nitrogen group, are shown together with TMTFA. (B, right) Closeup of the active site of the TMTFA−TcAChE complex, showing the experimentally determined TMTFA (open-face lines) with a superimposed model of ACh docked in the active site (solid lines).[9] Several key residues in the binding pocket are indicated.

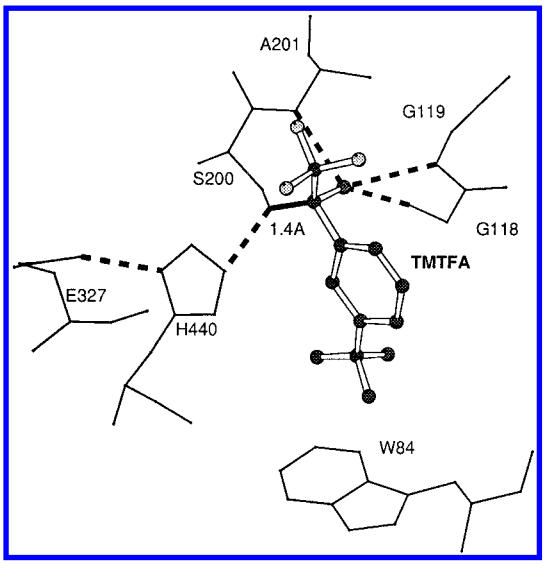

Figure 4. Closeup of the TMTFA−TcAChE complex showing its covalent bonding with S200. The amino acid side chains are shown as solid lines, TMTFA is shown as balls and sticks, and the covalent bond between TMTFA and S200 is shown as a bold line. The dashed lines denote hydrogen bonds to the putative residues in the oxyanion hole, i.e., G118, G119, and A201, and in the catalytic triad, i.e., S200, H440, and E327.

tion of the binding of 3-(octylthio)-1,1,1-trifluoropropan-2-one to *E. electricus* AChE, which showed that the inhibitor was bound in a tetrahedral adduct that was distinct from the ketone hydrate.[41] In Figure 4 the oxyanion of the tetrahedral adduct projects toward and hydrogen bonds with the peptidic NH functions of G118, G119, and A201, the respective O to N distances being 2.9, 2.9, and 3.2 Å. Thus, AChE possesses a three-pronged oxyanion hole, a more elaborate motif for stabilization of high-energy intermediates and transition states[53] than the two-pronged oxyanion holes of the serine proteases α-chymotrypsin,[54] trypsin,[55] and subtilisin.[56] Such a three-pronged oxyanion hole has also been reported for *Candida rugosa*[57] and *Rhizomucor miehei*[58,59] lipases, which like acetylcholinesterase are members of the α/β-hydrolase fold family of enzymes.[60] This putative tripronged oxyanion hole was earlier suggested on the basis of modeling the tetrahedral intermediates in the acylation stages of AChE-catalyzed hydrolyses of ACh[9] and ATCh.[25,26]

Solvent isotope effects on k_{cat}/K_m for AChE-catalyzed turnover of various substrates indicate that proton transfers contribute to transition state stabilization.[61−68] It is likely that the formation of the tetrahedral adduct described herein is ac-

(45) Schowen, K. B.; Smissman, E. E.; Stephen, W. F., Jr. *J. Med. Chem.* **1975**, *18*, 292−300.
(46) Smissman, E. E.; Nelson, W. L.; LaPidus, J. B.; Day, J. L. *J. Med. Chem.* **1966**, *9*, 458−465.
(47) Smissman, E. E.; Parker, G. R. *J. Med. Chem.* **1973**, *16*, 23−27.
(48) Stephen, W. F.; Smissman, E. E.; Schowen, K. B.; Self, G. W. *J. Med. Chem.* **1972**, *15*, 241−243.
(49) Sundaralingam, M. *Nature* **1968**, *217*, 35−37.
(50) Cushley, R. J.; Mautner, H. G. *Tetrahedron* **1970**, *26*, 2151−2159.
(51) Datta, N.; Mondal, P.; Pauling, P. *Acta Crystallogr., Sect. B* **1980**, *36*, 906−909.
(52) Partington, P.; Feeney, J.; Burgen, A. S. V. *Mol. Pharmacol.* **1972**, *8*, 269−277.
(53) Gerlt, J. A.; Gassman, P. G. *Biochemistry* **1993**, *32*, 11943−11952.
(54) Henderson, R. *J. Mol. Biol.* **1970**, *54*, 341−354.
(55) Marquart, M.; Walter, J.; Deisenhofer, J.; Bode, W.; Huber, R. *Acta Crystallogr., Sect. B* **1983**, *39*, 480−490.
(56) Robertus, J. D.; Kraut, J.; Alden, R. A.; Birktoft, J. J. *Biochemistry* **1972**, *11*, 4293−4303.
(57) Grochulski, P.; Bouthillier, F.; Kazlauskas, R. J.; Serreqi, A. N.; Schrag, J. D.; Ziomek, E.; Cygler, M. *Biochemistry* **1994**, *33*, 3494−3500.
(58) Brzozowski, A. M.; Derewenda, U.; Derewenda, Z. S.; Dodson, G. G., Lawson, D. M.; Turkenburg, J. P.; Bjorkling, F.; Huge-Jensen, B., Patkar, S. A.; Thim, L. *Nature* **1991**, *351*, 491−494.
(59) Derewenda, U.; Brzozowski, A. M.; Lawson, D. L.; Derewenda, Z. S. *Biochemistry* **1992**, *31*, 1532−1541.
(60) Ollis, D. L.; Cheah, E.; Cygler, M.; Dijkstra, B.; Frolow, F.; Franken, S. M.; Harel, M.; Remington, S. J.; Silman, I.; Schrag, J. D.; Sussman, J. L.; Verscheuren, K. H. G.; Goldman, A. *Protein Eng.* **1992**, *5*, 197−211.

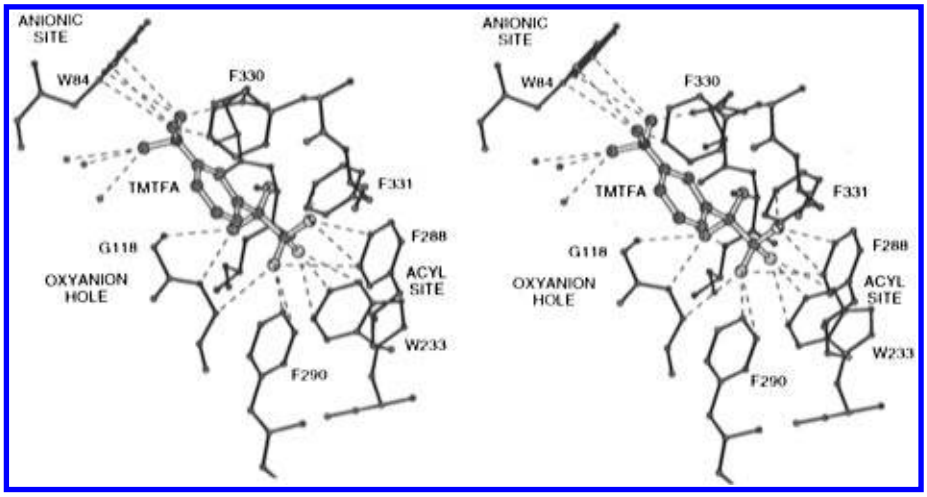

Figure 5. Stereoview of TMTFA in the active site of TcAChE. TheTMTFA model is denoted with black balls and thick gray bonds; the key amino acid residues in the active site are shown as black balls and thin black bonds. The dashed lines show the multiple close contacts with the "anionic" site, the oxyanion hole, and the acyl binding pocket.

companied by proton transfer from S200 to H440. In the adduct, $N^{\epsilon 2}$ of H440 points toward the O^{γ} of S200, which is covalently linked to the carbonyl carbon of TMTFA. The corresponding N to O distance is 2.7 Å, which suggests an NH to O hydrogen bond mimicking the S200 to H440 proton transfer which accompanies formation of the tetrahedral intermediate in the acylation stage of catalysis. This suggestion is supported by the NMR characterization of the tetrahedral transition state analog complex formed between the serine protease α-chymotrypsin and *N*-acetyl-L-leucyl-L-phenylalanyl trifluoromethyl ketone.[69] In this complex the active site histidine is in the histidinium ion form, which is still protonated at pH values as high as 10. Adebodun and Jordan[70] showed, by ^{31}P NMR, that the active site histidine in diisopropylphosphorylserine proteases titrates with a normal pK_a near 7.4. However, in the monoisopropylphosphorylserine proteases, which provide better models of the transition state, the apparent pK_a of the active site histidine ranges from 9.7 to 11.4. The pK_a values of active site histidines in serine proteases[10−13] and AChE[4] usually fall in the range of 6−7.5. The increased basicity of H440 in the tetrahedral transition state analog complex and, by analogy, in the tetrahedral intermediate is probably important for AChE catalysis, since the histidinium ion is stabilized. Amino acids which might contribute to this stabilization are the adjacent anionic residues E199 and E327. The E199Q mutant of TcAChE has a k_{cat}/K_m 50-fold lower than that of the wild type enzyme,[23] while the E327D and E327Q mutants of human AChE are inactive.[21]

One can also estimate the contribution of the triad residues to transition state stabilization from the results of site-directed mutagenesis experiments.[21] Single mutations to alanine of any one of the residues of the human AChE triad yield mutant enzymes with <0.0003-fold the activity of the wild type enzyme, while the S200C and E327D mutants have <0.003- and <0.004-fold the activity of the wild type enzyme, respectively. These effects on activity indicate that proton transfer catalysis provides 3−5 kcal mol^{-1}, or more, of transition state stabilization. The 5 kcal mol^{-1} estimate of transition state stabilization arising from mutations of triad residues to alanine is somewhat less than that calculated[44] for mutants of subtilisin:[71] 6 kcal mol^{-1} for D32A, 8 kcal mol^{-1} each for H64A and S221A. Since the AChE estimate is a lower limit, a more accurate assessment of the contribution of the triad waits on the determination of the Michaelis−Menten kinetic parameters of triad mutants.

Quaternary Ammonium Binding Locus. Figure 5 shows interactions of the quaternary ammonium function of TMTFA with the amino acid side chains of W84, E199, F330, and three water molecules. These residues generate a concave binding site that makes a close fit with the quaternary ammonium group. The closest distances of approach of nonhydrogenic atoms of the respective amino acid residues and of the quaternary ammonium group are 3.7, 3.5, and 4.0 Å, while the three water molecules are 3.2, 3.3, and 3.9 Å from it. This view of the quaternary ammonium binding locus is in agreement with various results in the literature. Modeling of the tetrahedral intermediates in the acylation stages of AChE-catalyzed hydrolyses of ACh[9] and ATCh[25,26] supports the role of these residues in molecular recognition. Site-directed mutagenesis of W84 to A in human AChE reduces k_{cat}/K_m by 3000-fold,[25] which is consistent with 4.7 kcal mol^{-1} of transition state stabilization arising from interaction between W84 and the quaternary ammonium function. The mouse AChE mutants Y330F and Y330A have k_{cat}/K_m values that are 2.3- and 6.5-fold lower than that of the wild type enzyme,[24] and therefore F330A has a 3-fold effect, which is consistent with 0.7 kcal mol^{-1} of transition state stabilization. The E199Q mutant of TcAChE has a 50-fold lower k_{cat}/K_m than does the wild type enzyme,[23] which corresponds to 2.3 kcal mol^{-1} of transition state stabilization. Therefore, if these contributions are additive, the residues of the quaternary ammonium binding locus contribute about 5×10^5 (or 8 kcal mol^{-1}) to the 10^{13}-fold catalytic acceleration of ACh hydrolysis effected by AChE. Nair *et al.*[43] constructed a quantitative structure−activity relationship (QSAR) for interaction of 10 *m*-substituted trifluoroacetophe-

(61) Pryor, A. N.; Selwood, T.; Leu, L.-S.; Andracki, M. A.; Lee, B. H.; Rao, M.; Rosenberry, T.; Doctor, B. P.; Silman, I.; Quinn, D. M. *J. Am. Chem. Soc.* **1992**, *114*, 3896−3900.
(62) Quinn, D. M.; Swanson, M. L. *J. Am. Chem. Soc.* **1984**, *106*, 1883−1884.
(63) Rosenberry, T. L. *Proc. Natl. Acad. Sci. U.S.A.* **1975**, *72*, 3834−3838.
(64) Acheson, S. A.; Barlow, P. N.; Lee, G. C.; Swanson, M. L.; Quinn, D. M. *J. Am. Chem. Soc.* **1987**, *109*, 246−252.
(65) Acheson, S. A.; Dedopoulou, D.; Quinn, D. M. *J. Am. Chem. Soc.* **1987**, *109*, 239−245.
(66) Barlow, P. N.; Acheson, S. A.; Swanson, M. L.; Quinn, D. M. *J. Am. Chem. Soc.* **1987**, *109*, 253−257.
(67) Acheson, S. A.; Quinn, D. M. *Biochim. Biophys. Acta* **1990**, *1040*, 199−205.
(68) Kovach, I. M.; Larson, M.; Schowen, R. L. *J. Am. Chem. Soc.* **1986**, *108*, 3054−3056.
(69) Liang, T.-C.; Abeles, R. H. *Biochemistry* **1987**, *26*, 7603−7608.
(70) Adebodun, F.; Jordan, F. *J. Cell. Biochem.* **1989**, *40*, 249−260.
(71) Carter P.; Wells, J. A. *Nature* **1988**, *332*, 564−568.

nones, including TMTFA, with TcAChE and *E. electricus* AChE. The salient features of the QSAR results were (a) induced London dispersion interactions with the *m*-substituents contribute to molecular recognition in the quaternary ammonium binding locus (b) the substituent-dependent range of transition state analog affinities was 10^7, of which 10^5 arises from interactions between the *m*-substituent and active site residues and 10^2 arises from inductive electronic effects on the stability of the hemiketal adduct between the inhibitors and S200. The 10^5-fold range is reasonably close to the effect computed above on the basis of the site-directed mutagenesis data. Recent molecular orbital calculations of the complexation of benzene and tetramethylammonium ion indicate that both cation$-\pi$ interactions and electron correlation effects contribute to the stability of the complex.[72] This view is shared by Dougherty and co-workers,[73,74] who have characterized the interactions of various organic cations (including tetraalkylammonium ions) with aromatic cyclophane hosts. Moreover, Ordentlich *et al*.[25] interpret the effect of the W84A mutation on the activity of human AChE in terms of cation$-\pi$ interactions between the quaternary ammonium group of substrates and W84. The transition state analog complex described herein provides a compelling structural rationale for these enzyme and ligand structure−function effects.

Acyl Binding Pocket. Modeling of ACh[17,18] and ATCh[25,26] in the acyl binding pocket of TcAChE and human AChE indicated that the binding pocket provides a tight fit for the acetyl group, thus providing a structural basis for the low activity of AChE on butyrylcholine and (butyrylthio)choline. This tight fit was provided largely by the aromatic rings of F288 and F290. Indeed, site-directed mutagenesis to L and V, respectively, the residues which are found at the same locus in butyrylcholinesterase, permitted the mutated TcAChE to hydrolyze (butyrylthio)-choline almost as well as ATCh.[17,18] Similar results have been obtained in mutagenesis experiments on mouse AChE[24] and human AChE.[25] Figure 5 shows that in the TMTFA−AChE complex the CF_3 group fits very snugly into a concave acyl binding pocket that consists of residues G119, W233, F288, F290, and F331. Hence, the structure of the complex is in substantial agreement with, and yet goes beyond, the above-cited molecular modeling and mutagenesis experiments. The closest distances of approach of fluorines of the CF_3 function to nonhydrogenic atoms of active site amino acid residues are 3.4 Å to F331, 3.3 Å to F290, 2.9 Å to F288, and 3.2 Å each to W233 and G119. Therefore, the closest approach of the CF_3 group is to F288, which is also in agreement with site-directed mutagenesis experiments. For example, the F288A mutant of human AChE has a 133-fold higher k_{cat}/K_m for (butyrylthio)-choline than does the native enzyme, but the corresponding change for the F290A mutant is only 5.6-fold.[25]

The homologous methyl analog of TMTFA, *m*-(*N*,*N*,*N*-trimethylammonio)acetophenone, is also an inhibitor of AChE ($K_i = 0.5\ \mu M$),[38] though binding to the enzyme is $>10^7$-fold weaker than that of TMTFA. The relative electrophilicities of the carbonyl carbons of the inhibitors nicely account for their relative binding affinities. TMTFA is an equilibrium mixture of the free ketone and ketone hydrate in aqueous solution, with a hydration equilibrium constant of 60 000.[42,43] The methyl homolog, in contrast, is hydrated to less than 1%.[38] Since hydration and covalent interaction with S200 of the active site both involve addition to the carbonyl carbon of oxygen nucleophiles, the relative hydration equilibria of the two inhibitors suggest that the electron-withdrawing character of the CF_3 group stabilizes the tetrahedral hemiketal adduct with S200. There is no need, therefore, to ascribe the tighter binding of TMTFA to better interactions of CF_3 than CH_3 with the residues of the acyl binding pocket. This assertion is supported by the fact that the molar refractivities, which measure the ability of a substituent to be involved in dispersion interactions, of CH_3 and CF_3 are nearly the same, while the hydrophobicity of CF_3 is only 1.6 times greater than that of CH_3.[75] Rather, the primary function of the acyl binding pocket of AChE is to present a sterically circumscribed concave binding surface to the substrate that accepts acetyl or propanoyl functions but excludes the larger butyryl function. This idea accords with the report that AChE catalyzes the hydrolysis of ATCh and (propanoylthio)choline via an S200−H440−E327 triad mechanism, but since (butanoylthio)choline and benzoylcholine do not fit into the acyl binding pocket, they cannot approach S200 and are consequently hydrolyzed by a cryptic mechanism that may involve E199.[26]

Conclusion. The TcAChE−TMTFA complex described in this paper provides the most intimate view to date of the intermolecular interactions at the active site that produce the enormous catalytic power of AChE. Of the 18 kcal mol^{-1} of transition state stabilization that AChE utilizes to effect catalysis, 11−13 kcal mol^{-1} come from interactions in the quaternary ammonium binding locus and the functioning of the S200−H440−E327 triad. The residual 5−7 kcal mol^{-1} of transition state binding energy probably comes from interactions of the incipient oxyanion of ACh with the tripartite oxyanion hole. The energetics of interaction in the oxyanion hole of α-chymotrypsin provide a precedent for this assignment. The pK_a of the hemiketal hydroxyl in the complex of α-chymotrypsin and *N*-acetyl-L-leucyl-L-phenylalanyl trifluoromethyl ketone is 4.2 units lower than the pK_a of model hemiketals.[69] This pK_a reduction corresponds to a 5.7 kcal mol^{-1} stabilization of the hemiketal oxyanion on binding to the active site, and presumably arises from H-bonding and electrostatic interactions in the oxyanion hole. Bencsura *et al*.[76] estimated by molecular mechanics that interaction with the oxyanion hole stabilizes a phosphoryl function in the AChE active site by ∼6 kcal mol^{-1}. Our estimate of transition state binding energy provided by the oxyanion hole is in substantial agreement with these literature values for transition state analog binding to serine enzymes.

The AChE active site provides an interaction surface that is complimentary to the extended conformation of ACh, of which TMTFA is a constrained mimic. The CF_3 group of TMTFA occupies an acyl binding pocket that is comprised of five convergent amino acid residues and that gives AChE its acetyl ester specificity. These structural elements of AChE catalytic power and substrate specificity accord nicely with the voluminous literature on this important enzyme. Four binding loci, the quaternary ammonium and acyl binding sites, the oxyanion hole, and the catalytic triad, converge on, envelop, and hence sequester TMTFA from solvent in the complex and, by analogy, ACh in the transition state. In fact, the formation of the TMTFA−TcAChE complex is accompanied by the displacement of six water molecules that are found in the native structure. The geometrical constraints thus invoked may be the reason why the active site of such a rapid enzyme is located deep within the enzyme molecule at the bottom of the aromatic gorge.

(72) Kim, K. S.; Lee, J. Y.; Lee, S. J.; Ha, T.-K.; Kim, D. H. *J. Am. Chem. Soc.* **1994**, *116*, 7399−7400.
(73) Dougherty, D. A.; Stauffer, D. A. *Science* **1990**, *250*, 1558−1560.
(74) Kearney, P. C.; Mizoue, L. S.; Kumpf, R. A.; Forman, J. E.; McCurdy, A.; Dougherty, D. A. *J. Am. Chem. Soc.* **1993**, *115*, 9907−9919.
(75) Hansch, C.; Leo, A. *Substituent Constants for Correlation Analysis in Chemistry and Biology*; John Wiley & Sons: New York, 1989.
(76) Bencsura, A.; Enyedy, I.; Kovach, I. M. *Biochemistry* **1995**, *34*, 8989.

A potential catalytic advantage that can arise from a buried active site is that the transition state forms in a "dry" environment. The ultimate of dry environments for transition states of chemical reactions is, of course, the gas phase. In this vein, the second-order rate constant for nucleophilic displacement of Br^- from CH_3Br by HO^- in the gas phase is 16 orders of magnitude larger than that in aqueous solution.[77] Addition of oxygen nucleophiles to carbonyl compounds has been studied both theoretically and experimentally.[78,79] Madura and Jorgensen compared the energetics of HO^- addition to formaldehyde in the gas phase and aqueous solution by quantum mechanical and statistical mechanical calculations.[78] In the gas phase, formation of the anionic tetrahedral adduct is exothermic by 35 kcal mol^{-1}. An ion−dipole complex whose formation is exothermic by 19 kcal mol^{-1} precedes the tetrahedral adduct and proceeds to the adduct over a small energy barrier, 1.1 kcal mol^{-1}.[78] These theoretical calculations agree with the estimate of Baer *et al.*[79] that formation of tetrahedral adducts from alkoxides and aldehydes is exothermic by 30 kcal mol^{-1}. The aqueous phase reaction, on the other hand, involves a transition state energy barrier of 24−28 kcal mol^{-1} and proceeds to a tetrahedral adduct that lies 10−14 kcal mol^{-1} above the reactants.[78] The dramatic difference in reaction energetics in the aqueous versus the gas phase reflects the differential strength of solvent−solute interactions in the reactants and transition state. Hence, the primary contribution to reaction barriers in solution, and thus to the slowness of aqueous phase reactions, is preferential solvation of reactants.[77,78] Because the buried active site of AChE provides an environment for the transition state that is intermediate between the aqueous and gas phases, one expects that the activation barriers for formation and decomposition of the tetrahedral intermediate will be decreased and the turnover rate correspondingly increased.

Materials and Methods

Synthesis of *m*-(*N*,*N*,*N*-Trimethylammonio)-2,2,2-trifluoroacetophenone, TMTFA. The iodide salt of TMTFA was synthesized as previously described.[42] The ^{19}F and ^1H NMR spectra and FTIR and mass spectra are consistent with the structure in Figure 1, as described previously.[42]

X-ray Structure. Crystalline TcAChE complexed with TMTFA was obtained by soaking native crystals of TcAChE for 12 days in a solution containing 2 mM TMTFA. Diffraction data were collected to 2.8 Å resolution on a Xentronics area detector. The structures were determined by the difference Fourier technique and refined by using simulated annealing and restrained refinement using X-PLOR,[80] as described previously.[9,19]

The overall conformations of native TcAChE and of the TcAChE−TMTFA complex are very similar, with an rms deviation of only 0.4 Å between equivalent C_α positions. The highest positive peak (7σ) of electron density in the difference Fourier map is within a covalent bonding distance of S200O$^\gamma$, and its shape accommodates a TMTFA molecule (cf. Figure 2). A model of TMTFA was generated by using the EDR coordinates[19] to build the trimethylammoniophenyl fragment, and the ACh coordinates[81] to build the trifluoroaceto fragment, albeit with the C−F distance adjusted to 1.5 Å. The final refinement parameters are R factor 0.188, $R_{free} = 0.235$, number of water molecules 99, number of sulfate molecules 1, rms bond 0.012 Å, rms angle 1.756°.

The TMTFA molecule occupies the position of six water molecules that are found in the 2.25 Å native structure (Harel et al. Manuscript in preparation). Upon binding to TMTFA, the S200O$^\gamma$ swings from its position in the native structure to become a partner in the tetrahedral conformation at a distance of 1.4 Å from the aceto C (cf. Figure 4). It is important to note that this is a result of the refinement, as this bond distance was not restrained.

Coordinates of the final model of the TcAChE−TMTFA complex and experimental structure factor amplitudes (for the 2.8 Å data set) have been deposited with the Brookhaven Protein Data Bank,[82] with ID Codes 1AMN and R1AMNSF, respectively.

Acknowledgment. We thank Lilly Toker for preparation of the *Torpedo* AChE and Alexander Faibusovitch and Clifford Felder for help in the computation. This research was supported by the U.S. Army Medical, Research and Development Command under Contract No. DAMD17-93-C-3070, the Association Franco-Israélienne pour la Recherche Scientifique et Technologique (AFIRST), the Minerva Foundation, Munich, Germany, the Kimmelman Center for Biomolecular Structure and Assembly, Rehovot, and NIH Grant NS21334 (to D.M.Q.).

JA952232H

(77) Bohme, D. K.; Mackay, G. I. *J. Am. Chem. Soc.* **1981**, *103*, 978−979.

(78) Madura, J. D.; Jorgensen, W. L. *J. Am. Chem. Soc.* **1986**, *108*, 2517−2527.

(79) Baer, S.; Brinkman, E. A.; Brauman, J. I. *J. Am. Chem. Soc.* **1991**, *113*, 805−812.

(80) Brünger, A. T. *X-PLOR Version 3.1, A System for Crystallography and NMR*; Yale University Press: New Haven and London, 1992; 3.1 Manual.

(81) Chothia, C.; Pauling, P. *Nature* **1968**, *290*, 1156−1157.

(82) Bernstein, F. C.; Koetzle, T. F.; Williams, G. J. B.; Meyer, E. F., Jr.; Brice, M. D.; Rodgers, J. R.; Kennard, O.; Shimanouchi, T.; Tasumi, M. *J. Mol. Biol.* **1977**, *112*, 535−542.